Early detection of hand movements from electroencephalograms for stroke therapy applications

Early detection of hand movements from electroencephalograms for stroke therapy applications

A Muralidharan[1,2], J Chae[1,2,3] and D M Taylor[1,2,4,5]

[1] Department of Biomedical Engineering, Case Western Reserve University, Cleveland, OH 44106, USA
[2] Cleveland Functional Electrical Stimulation (FES) Center of Excellence, Louis Stokes VA Medical Center, Cleveland, OH 44106, USA
[3] Department of Physical Medicine and Rehabilitation, Case Western Reserve University at MetroHealth Medical Center, Cleveland, OH 44109, USA
[4] Department of Neurosciences, The Cleveland Clinic, Cleveland, OH 44195, USA
[5] Department of Orthopaedics, MetroHealth Medical Center, Cleveland, OH 44109, USA

E-mail: dawn.taylor@case.edu

Abstract

Movement-assist devices such as neuromuscular stimulation systems can be used to generate movements in people with chronic hand paralysis due to stroke. If detectable, motor planning activity in the cortex could be used in real time to trigger a movement-assist device and restore a person's ability to perform many of the activities of daily living. Additionally, re-coupling motor planning in the cortex with assisted movement generation in the periphery may provide an even greater benefit—strengthening relevant synaptic connections over time to promote natural motor recovery. This study examined the potential for using electroencephalograms (EEGs) as a means of rapidly detecting the intent to open the hand during movement planning in individuals with moderate chronic hand paralysis following a subcortical ischemic stroke. On average, attempts to open the hand could be detected from EEGs approximately 100–500 ms *prior* to the first signs of movement onset. This earlier detection would minimize device activation delays and allow for tighter coupling between initial formation of the motor plan in the cortex and augmentation of that plan in the periphery by a movement-assist device. This tight temporal coupling may be important or even essential for strengthening synaptic connections and enhancing natural motor recovery.

(Some figures in this article are in colour only in the electronic version)

1. Introduction

Each year, approximately 795 000 Americans experience a new or recurrent stroke. Many stroke survivors are left with chronic motor, sensory and cognitive impairments, making stroke the leading cause of serious long-term disability in the United States [1]. Common deficits after a stroke affecting the motor areas of the brain include muscle weakness, spasticity, and problems with joint coordination, dexterity and movement precision. The middle cerebral artery stroke is the most common non-hemorrhagic stroke, which preferentially affects the upper limb [2]. This loss of upper-limb function substantially limits one's ability to perform the basic activities of daily living.

Some natural recovery of motor function usually occurs in the first few months following a stroke. Therapies that encourage or require voluntary, repetitive and functionally relevant use of the affected limb have been shown to be effective in enhancing motor recovery even years after a stroke [3, 4]. Strategies, such as constraining one's unaffected limb, force individuals to attempt daily tasks with their affected limb to further encourage motor recovery [5]. However, in

Table 1. Study participant information. All participants were right-hand dominant prior to their stroke. Fugl–Meyer scores for normal wrist and hand function are 10 and 14, respectively [22].

Subject	Time post stroke	Hemisphere of stroke	Data used to determine movement onset	Fugl–Meyer score	
				Wrist	Hand
1	2y 10 mo	Right	EMG	7	7
2	7y 0 mo	Left	Bend sensor	5	10
3	11 mo	Right	EMG	7	10
4	2y 1.5 mo	Left	Bend sensor	7	13

spite of these available therapies, many individuals are left with some chronic hand paralysis even after the rest of the limb has regained significant function.

Several types of devices are being developed to generate or augment hand movements in people with paralysis. For example, neuromuscular stimulation systems can generate hand movements by electrically activating the peripheral nerves to the paralyzed muscles [6, 7] and motorized exoskeletons can restore function by moving the paralyzed hand directly [8–10]. These movement-assist devices can help people with partial or complete chronic hand paralysis perform more of the activities of daily living. Movement-assist devices may also improve therapeutic outcomes following stroke by facilitating repetitive practice of functional tasks.

Repetitive, voluntary and functionally relevant movements are thought to promote recovery of motor function through use-dependent plasticity. With repetitive-movement therapies, task-specific synaptic connections are strengthened over time due to coordinated and repeated activation of the pre- and post-synaptic neurons throughout the sensorimotor pathways. This activity-dependent motor relearning is thought to occur through Hebbian mechanisms, which are strongly affected by the intensity and relative timing of activity in the pre- and post-synaptic neurons [11–16].

Studies have shown two key aspects of timing that affect synaptic plasticity. First, 'causal' timing (where the pre-synaptic neurons fire before the post-synaptic neurons) results in an increase in the strength of a synapse. Second, this increase in synaptic strength is highly dependent on how closely in time the pre- and post-synaptic cells fire. The closer in time the two cells fire, the greater the effect this firing has on changing the strength of the synapse [11–16].

The tight causal timing required to maximize Hebbian plasticity may impact the effectiveness of different movement therapy strategies after stroke, especially when a movement-assist device is used to generate or augment movements. For a movement-assist device to be used, the device has to receive and interpret a signal telling it what movement the person is trying to make. Then the device has to generate an appropriate action in the limb. Both of these processing steps can take time, resulting in a longer-than-normal delay between motor planning in the cortex and execution of that plan in the periphery. This long delay may limit the therapeutic gains from using a movement-assist device.

For people who are only moderately impaired, residual-muscle activity or small movements can be detected and used to trigger a device that will augment those very same movements. In this case, the device can only be activated after peripheral signs of movement have already started. Alternatively, characteristic changes in brain activity are known to occur prior to movement onset throughout the parietal, supplementary motor, premotor and primary motor cortices. Extracting one's intended movements directly from the cortex *before* movement onset may be a viable option for reducing these time delays and tightly linking motor planning in the cortex with execution in the periphery. For individuals with complete hand paralysis, detecting intent to move from the cortex may be the only natural option for triggering a movement-assist device.

Most EEG-based brain–machine interface studies evaluate able-bodied individuals or individuals paralyzed due to spinal cord injury or amyotrophic lateral sclerosis. So far, only a few groups besides ours have focused on detecting hand movements from EEG in the stroke population where the damage is in the brain itself [17–20]. None of these other stroke studies assess the ability to detect intent to move specifically during the motor planning phase *prior* to the earliest time that movement could be detected in the periphery. In this study, our group uniquely focused on early detection in this very narrow and challenging pre-movement time window. We developed a process to identify signal processing and classification parameters that optimize the balance between the speed and accuracy of detection in order to maximize early detection. We focused on this brief pre-movement time window for two reasons. First, reducing time delays in triggering device-assisted movements will result in more natural movements and could potentially enhance beneficial plasticity by more closely restoring the natural timing between cortical intent and the movement assistance in the periphery. Second, the muscle activity or the finger motion itself could be used as a reliable device trigger in this moderately impaired stroke population once the actual movement has started. Therefore, later movement detection from EEGs is not as clinically useful in this population.

2. Methods

2.1. Experimental design

Four individuals with moderate chronic hand paralysis participated in this study. All participants previously had a subcortical ischemic stroke and were left with a limited ability to voluntarily extend their fingers. Specifically, participants exhibited at least some volitional finger extension, but strength

was four or less on the Medical Research Council scale [21]. Table 1 indicates time since the stroke, the hemisphere in which the stroke occurred, the scores for wrist and finger function from the Fugl–Meyer assessment[6] [22], and if bend sensor or electromyographic (EMG) data were used to determine onset of movement for that participant. All participants came in for testing on four different days over a four week period. The study protocol was approved by MetroHealth Medical Center's Institutional Review Board.

During each session, participants were seated in front of a computer screen with both forearms resting comfortably on a padded table. Visual cues to open or relax either the affected or unaffected hand were presented on the computer screen. Participants were instructed to attempt to maintain active extension of the fingers throughout the hand-open cue and to simply relax the hand and allow the hand to close naturally during the relax cue. Each 'trial' consisted of relaxing both hands for 5 s followed by a cue to actively extend the fingers of the right or left hand for 5 s. Cues were presented in random order in blocks of up to 20 movement cues per block. Participants were encouraged to take breaks between blocks to prevent fatigue. Each day's testing session was analyzed separately.

2.2. Data collection

Thirty-two gold cup EEG electrodes spanning the sensorimotor areas were attached to the scalp with conductive paste (locations approximately corresponding to a rectangular grid spanning F3 through CP4 in the 10–5 system [23]). Bipolar EMG sensors were placed on the forearms over the finger extensor muscles (extensor digitorum communis). Flexible bend sensors (electrogoniometer from Biometrics, UK) were taped along the dorsal surface of the index fingers spanning the first proximal knuckle. These bend sensors put out a voltage proportional to the angle of the proximal finger joint. Bend sensor, EMG and EEG voltages were recorded simultaneously at 610 Hz using a 64-channel recording system (Pentusa RX5, Tucker Davis Technologies, FL). The digital EEG and EMG signals were bandpass filtered to 2–150 Hz with an additional notch filter at 60 Hz.

Visual cues to open/relax either the right or left hand were presented on a computer screen and controlled by Matlab (Mathworks). Changes in the hand cue state were accompanied in real time by changes in a digital cue code sent from Matlab to the recording system. This hand movement cue code was synchronized and integrated with the digitized EEG, EMG and bend sensor data file. All of these data were then down sampled to 305 Hz for further processing.

Additional processing was done to obtain cue data, hand movement data and features of the EEG used to predict movement onset in 100 ms intervals. Specifically, differential EMG data were rectified and averaged over each 100 ms window. Bend sensor voltage data were simply down sampled to 10 Hz. Power was calculated via fast Fourier transforms (FFT) from the EEGs every 100 ms using overlapping
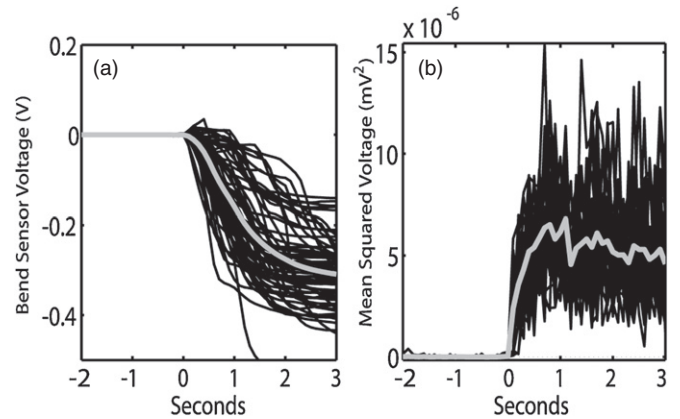
Figure 1. Examples of bend sensor and EMG data from all trials within a session aligned at movement onset ($t = 0$). The thicker gray line shows mean values. (a) Bend-sensor data from one participant. Note that movement in either the flexed or extended direction qualified as movement onset. (b) EMG data from a different participant.

windows of data (FFT window length was varied as part of the optimization process described below). The resulting 10 Hz sampling rate for all the processed data allowed for new movement predictions to be made every 100 ms, which is a movement update rate that can be accommodated by most simple movement-assist devices.

Rectified EMG or bend sensor data were used to determine actual movement onset times[7]. Cue onset and movement onset were used as key landmarks for aligning the data from each trial for later analysis. Figure 1 shows examples of bend sensor and EMG data from each trial aligned on movement onset. Movement onset was determined by a sustained change in sensor value over the range seen during the prior 2 s of the relaxed state. Note that the change in bend sensor value can either be positive or negative because some participants would, at times, briefly flex their fingers first as they tried to generate finger extension (see figure 1(a)). Since our goal was to identify attempted movements from the EEG prior to any actual movement, all time points that could reasonably be interpreted as part of the movement phase were labeled as such. This approach ensured that only EEG data before detectable movement onset were used in our pre-movement analysis.

2.3. Data analysis

Classifiers for the early detection of attempted finger extension of the affected hand were generated and assessed for each session using only the movement trials where the affected hand was cued to move (mean of 42 ± 12 trials per session). Classifiers were developed in two phases. The goal of the first phase was to identify combinations of specific EEG features

---

[6] The Fugl–Meyer assessment is used to quantify isolated and synergistic voluntary-motor function.

[7] In two of the participants, the EMG signals had low signal-to-noise ratios due to weak muscles and excess superficial fat in the arms. In those two participants, the bend sensor data were used to determine movement onset because they provided a more reliable, clear-cut indication of the start of movement.
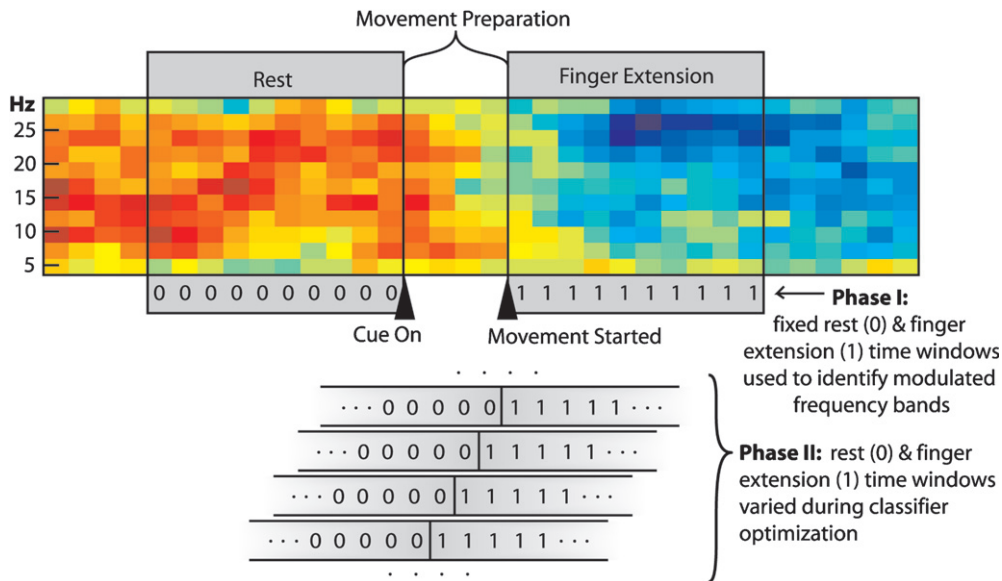
Figure 2. Spectrogram from one channel of EEG showing the epochs used in the different stages of analysis (red = higher power; blue = lower power). Triangles indicate the initial presentation of the hand-open cue and movement onset. The two gray boxes spanning the spectrogram indicate the two 1 s time segments used in phase I of the analysis (i.e. the relaxed (0) and finger extension (1) epochs). Analysis in phase II emphasized early detection of finger extension during the 'movement-preparation' epoch. The lower part of the figure shows how the assigned rest/finger-extension transition point (0 to 1) was systematically shifted across the movement preparation epoch in phase II as part of the process of optimizing an early detection classifier.

that modulate the most with finger extension of the affected hand. The goal of the second phase was to maximize early detection of movement onset using the best set of EEG features identified in phase one. These two phases used two distinct epochs of the EEG data.

2.3.1. Phase I analysis: identification of EEG features modulated with finger extension. Phase I analysis used data that were clearly in either the relaxed epoch or the finger-extension epoch to first identify which EEG features were significantly modulated with finger extension (see figure 2). Approximately 1 s of data from the relaxed epoch just prior to cue presentation and 1 s of data starting at movement onset were used from each trial for phase I analysis. The raw EEG signals from the extracted epochs were common average referenced to produce 32 new signals with common noise removed. In addition, common spatial pattern analysis [24–26] was also applied to the raw EEGs to derive 32 additional signals, each of which was a weighted sum of the original raw EEG signals. Common spatial pattern analysis has been shown to generate linear combinations of signals that maximize the difference in signal variance between two states [24–26]: in this case the finger extension versus the relaxed state.

FFTs were then applied to each of these 64 processed EEG signals to extract power features from each epoch for analysis. 128-sample FFTs were calculated, resulting in power bands of 2.38 Hz width. Because the recording hardware itself filtered out signals below 2 Hz, the lowest power band was discarded. The next highest 11 bands spanning the 2.38–28.59 Hz range were analyzed to determine which bands from which signals changed the amplitude between the relaxed versus finger-extension states. Multiple sliding 128-sample windows were

used to generate 10 power spectrum estimates per trial at even intervals across each 1 s epoch. Linear regression was used to predict the hand state from each power band from each signal individually in a 10×10 fold cross-validation process. Cross-validation results were used to identify which specific power features showed significant modulation with the finger-extension versus rest epochs at the 95% confidence level. We further verified that these power features had the appropriate decrease in power with attempted finger extension and increase in power with relaxation (and not the other way around). This check was done to ensure there were no significant scalp EMG artifacts associated with the attempted movement.

After this initial screening to identify EEG power features that were modulated with attempted movement, backward feature elimination [27, 28] was used to identify a reduced number of significant features that together convey the most robust information about the relaxed versus finger-extension epochs. Linear regression with five-fold cross-validation was used to drop features during the backward feature elimination process.

2.3.2. Phase II analysis: parameter optimization for early transition detection. While phase I identified combinations of EEG features that showed significant changes between the relaxed and extended finger states, phase II focused on using these features for the early detection of the transition from the relaxed to the extended finger state during movement-preparation (see figure 2). In phase II, three key signal processing parameters were optimized using the best combinations of features identified in phase I. These key parameters were: (1) window size used to calculate the FFT, (2) the number of sequential past and current power

Table 2. Values of the three signal processing/classification parameters tested during phase II.

Parameter	Parameter values tested
FFT window length[a]	100, 300, 500, 700 and 900 ms
Number of preceding processed data samples (at 10 Hz) used to predict present hand state	0 (current time sample only), 2, 4, or 6
Presumed transition point between the relaxed (0) and finger-extension state (1) used for training the classifier (see bottom of figure 2 showing state labels transitioning from 0 to 1 at different time points in the movement preparation epoch)	To be thorough, all transition points ranging from 1.2 s before to 0.5 s after movement onset were tested in 100 ms increments

[a] FFTs were still calculated every 100 ms using overlapping windows of data. Although changing window lengths altered the frequency band sizes, the frequency bands used for decoding were kept consistent with those identified in phase I by interpolating across bands as needed.

calculations used by the classifier to predict the current hand state, and (3) the presumed transition point on which to train the classifier (i.e. at what point in the movement preparation epoch do we define as the switch between the rest (0) versus finger extension (1) state for the purpose of training an early detection classifier). Properly optimizing these three parameters for each participant is critical because their values determine the balance between speed and accuracy of detection. For example, using longer overlapping windows of data for FFT calculation will increase the frequency resolution, which can improve movement detection; however, these longer time windows will also create a longer lag between the time the EEG power changes and when the FFT calculation fully reflects that change. Optimal combinations of these parameters were identified for each person by testing each possible combination of these three parameters over the ranges listed in table 2.

2.4. Classification and final performance measures from phase II

The early movement prediction performance was assessed for each of the above parameter combinations from table 2, to identify which combinations maximized the ability to predict finger extension during the motor planning prior to movement onset. Linear discriminant analysis was used to build classifiers with data from training trials and then test classification accuracy on separate testing trials in a leave-one-trial-out cross-validation process. Time points used for building the classifiers from training trials differed slightly from the time points used for assessing performance in the testing trials. This difference was necessary to ensure the classifiers were built using enough data from each movement state to prevent over fitting, while still assessing performance over the actual more-limited movement preparation window.

When training the classifier, 5 s of data (50 time points) uniformly spanning the presumed relax/move transition point were used from each trial regardless of where this transition point fell (recall this assumed transition point for training the classifier was one the parameters varied as part of the classifier optimization process as described in table 2). Specifically, for the sake of training each version of the classifier, 2.5 s or 25 time points from before the transition point were assigned to the relaxed state, and 2.5 s or 25 time points from the assumed transition point and beyond were assigned to the finger-extension state.

However, when assessing each classifier's performance, time samples of processed data assessed from each testing trial spanned 1 s (i.e. 10 time steps) before the cue through to the last time step before movement onset[8]. False-positive rates were calculated as the percentage of the rest epoch time points incorrectly classified as finger extensions, and true-positive rates were calculated as the percentage of time points during the actual movement preparation phase correctly classified as finger extension (movement preparation samples spanned the first time sample after the cue to the last time sample before detectable movement onset). The final overall performance measure for each parameter combination was calculated as the 'adjusted' true-positive rate (i.e. mean true-positive minus false-positive rate). This adjusted true-positive rate was used as the cost function to determine which combination of parameters from table 2 maximized this difference.

2.4.1. Performance at controlled false-positive rates.
Linear discriminant analysis identifies a linear combination of the signal features, which maximizes the difference between two states while minimizing the variance within each state. The classifier outputs a single scalar value at each time step, and that time point is defined as either being in the rest state or the finger-extension state based on whether the scalar output of the classifier is above or below a predefined threshold. With standard linear discriminant analysis, this threshold is set in a way that maximizes the correct classification of the most time points. However, this threshold can be shifted as needed to change the sensitivity of the classifier and make it more or less difficult to classify a time point as finger extension.

In stroke-therapy applications, the classification threshold can be shifted to reduce false triggers of a therapeutic device when a person is resting. However, this comes at the expense of also making the system less responsive to true triggers when a person is trying to move. Conversely, shifting the threshold to make a therapeutic device respond more reliably to attempted movements may come with a price of accepting some additional unintended false triggers.

---

[8] Classifiers were applied offline at each time step in the assessment window in the same manner as they would be if the data were being collected and used in real time. Therefore, classifiers that use additional time steps of past data to predict movement state in the current time step made use of some data that preceded the designated assessment window.
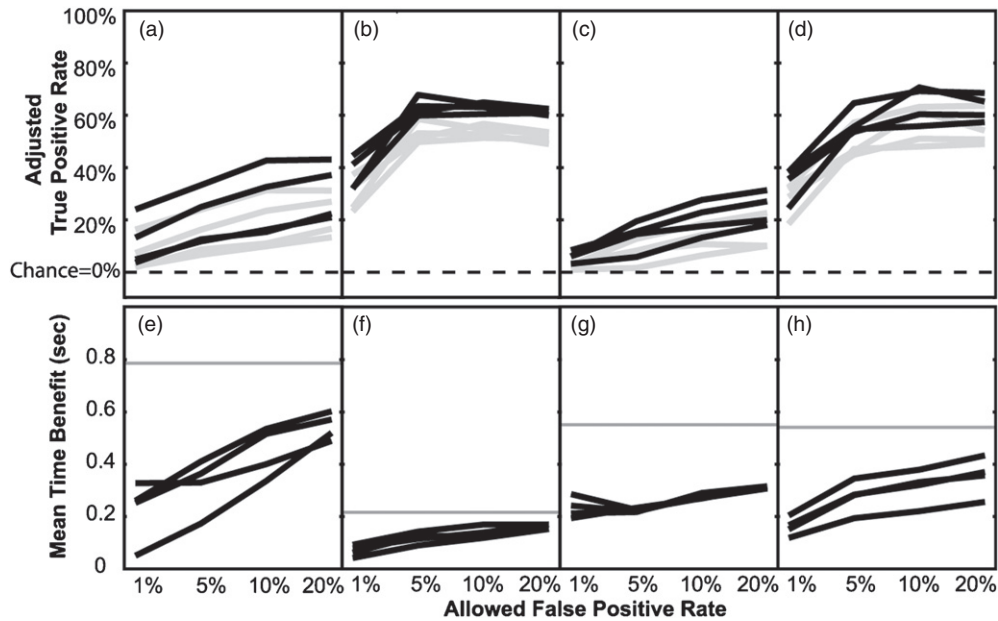
Figure 3. Adjusted true-positive rate and mean time benefit as a function of allowed false-positive rate. (a)–(d) Adjusted true-positive rates plotted separately for participants one through four (i.e. true-positive rate during the movement-preparation phase minus the false-positive rate during the rest phase. Note chance level = 0% and is indicated by the dotted lines). Within each graph, each black line indicates a different testing session, and gray lines indicate the lower 95% confidence intervals for each session. (e)–(h) Corresponding average time benefit of using EEGs to trigger a device over using EMGs or bend sensor data alone. In (e)–(h), gray lines indicate the maximum possible time benefit based on the length of each person's movement preparation time.

Since the therapeutic advantages are still unknown regarding increasing/decreasing the sensitivity of an EEG-triggered movement-assist device, performance was evaluated at four different thresholds or sensitivity levels. Thresholds were adjusted to produce 1, 5, 10 or 20% false positive samples during the rest epochs prior to cue presentation. The corresponding true-positive rates were calculated at each classification threshold. 'Adjusted' true-positive rates were then calculated as the true-positive rates minus the false-positive rates for the four threshold sensitivity settings.

3. Results

The adjusted true-positive rates for each allowed false-positive rate are shown for each person in figures 3(a)–(d). Each black line indicates a different testing session. Since the plotted adjusted true-positive rates already have the corresponding false-positive rates subtracted out, the expected random chance value for these data is zero because random data will generate equal true- and false-positive rates. This zero chance level holds true regardless of the classification threshold used.

The increase in adjusted true-positive rates at the higher false-positive rates indicates that allowing some false positives can pay off by disproportionally increasing the difference between the true- and false-positive rates. In all participants, attempted finger extension could be identified well above chance levels during movement preparation prior to detection of movement onset in the periphery. *P*-values ranged from $P < 0.2 \times 10^{-4}$ to $P < 3.7 \times 10^{-9}$ across people and sessions[9].

[9] Calculated via a one-tailed Wilcoxon signed rank test for each session at optimal decoding parameters using the default classification thresholds from linear discriminant analysis.

However, as the threshold for classifying a time sample as a finger extension event became more strict, the difference between the true- and false-positive rates dropped. The gray lines in figures 3(a)–(d) show the lower 95% confidence intervals of the adjusted true-positive rates calculated at each allowed false-positive rate (calculated via a bootstrap method [29, 30]). The lower 95% confidence interval came close to zero (chance level) in one or more sessions when the false-positive rate was reduced to 1% in participant one and when the false-positive rate was reduced to 1% or 5% in participant three.

The average time benefit of using EEGs for detecting movement onset over using EMG or bend sensor data alone is shown in figures 3(e)–(h). Average time benefit is calculated here as the average time difference between when the classifier first determined a finger-extension event has occurred during the movement preparation phase and when the actual movement was detected via EMGs or bend sensors. To minimize the contributions of false triggers to the time-benefit calculation, only time points 100 ms or more after the cue were used (time points classified as finger extension during rest or less than 100 ms after the cue were ignored, so they did not artificially inflate the calculated time benefit).

In this study, the EMG and/or bend sensor data were analyzed offline. Therefore, the first detectable sign of movement from EMGs or bend sensors could be rigorously identified for each trial by looking at the whole trial to spot when sustained changes in sensor values initially started. This manual inspection of each trial was needed because of variability within and between trials in the baseline sensor values in the rest phase (i.e. the hand did not always go back

to exactly the same position while relaxing; note in figure 1, baseline differences between trials have been subtracted out). However, reliably detecting movement onset from the EMGs or bend sensors in real time would likely require at least one to several additional time samples of data to be relatively certain the change in sensor value represented a real and sustained change from the previous value (i.e. not simply the result of noise or non-stationarities). Therefore, the actual time benefit of using EEGs is likely to be at least one hundred to several hundred milliseconds greater than the values shown in figures 3(e)–(h).

The participants had differences in the speed with which they were able to initiate a movement after the cue. People who take a long time to generate detectable muscle or joint activity in the periphery could potentially benefit more by using EEGs over EMGs/bend sensors than someone where the peripheral signs of movement start rather quickly in the movement generation process. The gray lines in figures 3(e)–(h) indicate the average maximum time benefit possible for each person based on how long it typically took them to generate peripheral signs of movement. This maximum possible time benefit was calculated as the time from 100 ms after the cue to mean onset of movement as measured by EMG or bend sensor data.

4. Discussion

Many brain–machine interface research labs have developed algorithms for detecting different hand movement states from EEGs in able-bodied individuals and in individuals with a spinal cord injury or with locked-in syndrome due to amyotrophic lateral sclerosis. These EEG-based brain–machine interface studies have generally produced mixed results. An estimated 20% of the people being tested in any given study typically cannot generate an effective control signal from their EEGs [31]. Here we have taken on the additional challenge of trying to detect attempted hand movements from EEGs using just a very short time window prior to actual movement onset in people who have some chronic hand paralysis due to stroke.

Our results show that attempted finger extension could be detected significantly above chance during the narrow movement preparation phase in all four stroke survivors tested here. However, accuracy rates differed across individuals, just like researchers have found in other populations. Perfect accuracy may not be needed to provide a benefit in the moderately impaired stroke population. Residual movements or EMGs could be used as a backup trigger if the impending movement failed to be detected from the EEGs during the movement preparation window. Earlier triggering of a movement assist device in at least some portion of the attempted movement may still improve the therapeutic benefits over EMG- or bend-sensor-based triggering alone. Early device triggering will more tightly couple the motor planning at the level of the cortex, with the motor action at the periphery, thus potentially augmenting Hebbian plasticity and motor relearning.

This study focused on evaluating early detection of the transition from the relaxed state to the fingers-extended state. It did not address the transition from the fingers-extended state back to the relaxed state. Initial testing showed most participants unintentionally started relaxing while the extend-fingers cue was still on. Once they saw the relax cue and realized they were already relaxed, they would re-extend the fingers once more so that they could then re-relax in response to the relax cue. These inconsistencies in the data collected during the extend-to-relax transition made it impossible to use this particular set of data to evaluate how reliably extend-to-relax transitions can be detected. (We are currently addressing problems with attention maintained in a separate study evaluating alternative cue presentation methods designed to keep people focused on the task.)

In real-time therapeutic applications, the hand state classifiers could be used as either an all-or-nothing movement command, or used in a more probabilistic integrative fashion. For example, a movement-assist device could be activated in an all-or-nothing manner by implementing a complete finger extension program whenever the device detected a 'finger extension command' while the hand was in the rest state. In this type of system, the classification threshold should be shifted to limit false positives because any false positive would produce full finger extension. However, this study showed that adjusting the threshold to reduce false positives can also disproportionately reduce the true-positive rate. In two of the four study participants, finger extension could still be detected during movement planning in 30–40% of the trials, even when false trigger rates were reduced to 1% (participants two and four). These individuals may benefit from the all-or-nothing EEG-based device triggering system even though the EEGs provide a time benefit in only 30–40% of the trials. However, reducing the false positives to 1% or less would nearly eliminate most true positives in the other two participants (participants one and three), thus substantially reducing any therapeutic benefit over EMGs or bend sensors alone.

Alternatively, a movement-assist device could be used in a more graded 'integrative' fashion. When using the classifier output in an integrative mode, the threshold should be set to maximize the *difference* between the true- and false-positive rates. For example, with a neuromuscular-stimulation system, each time sample classified as a finger-extension event could increase the current to the finger extensor muscles, whereas rest classification events would decrease the current. Under this probabilistic option, individuals with more correctly classified time samples than incorrectly classified time samples will, on average, build up stimulation when they are trying to open the hand and reduce stimulation when they are relaxing. This added stimulation could augment function, making the hand easier to open/close than without EEG-triggered stimulation.

All four study participants could potentially use an EEG-driven stimulation device in an integrative manner, because all four had substantive differences in the true- and false-positive rates at some classification thresholds. However, the gradual nature of the build up or reduction of stimulation when EEG triggers are used in an integrative mode will likely reduce the

time benefits of using EEGs over using EMGs or bend sensors alone. Online tests are needed to determine the therapeutic benefits of using a device in a more graded probabilistic fashion versus triggering a device in a rapid all-or-nothing manner, given the various true- and false-positive rates seen here at the different threshold settings.

Although each person's cortical motor planning patterns appeared to be relatively stable from day to day, there will likely be some variability in EEGs between sessions due to differences in the quality of the connection between the electrodes and the scalp each time the EEG electrodes are applied. Changes in medication and alertness level between days can also cause overall changes in the EEG power spectrum, even when the underlying motor planning patterns remain constant. Therefore, in the real-world use of an EEG-triggered movement-assist device, it is likely that at least some daily refinement of the classifier would be beneficial to account for any non-stationarities in the power spectrum or in the signal quality. Streamlining this refinement process will be important to make these systems practical for daily use. This process will likely entail normalizing the power features by subtracting out any baseline shifts as well as reweighting power features in the classifier that have become noisy or problematic.

During actual use of a brain-triggered movement-assist device, visual and tactile feedback of the resulting movements could help train users to generate stronger, more-consistent cortical activation patterns with practice. The cortical patterns required to trigger the device could even be gradually altered over time, thus encouraging the user to make even stronger or more 'normal' cortical activation patterns as they progress with their therapy. Results from this offline analysis suggest that the EEG signals in these moderately impaired stroke survivors contain enough hand movement information to trigger a movement-assist device, even if device activation is not 100% reliable. Feedback from this initial performance can then allow a person to learn to strengthen or improve their cortical activation patterns over time. Online tests are now needed to determine how much cortical patterns can be improved with feedback and if improved cortical patterns will result in greater functional recovery.

Acknowledgments

References

[1] Lloyd-Jones D *et al* 2009 Heart disease and stroke statistics—2009 update: a report from the American Heart Association Statistics Committee and Stroke Statistics Subcommittee *Circulation* **119** e21–181

[2] Dobkin B H 2004 Strategies for stroke rehabilitation *Lancet Neurol.* **3** 528–36

[3] Taub E *et al* 1993 Technique to improve chronic motor deficit after stroke *Arch. Phys. Med. Rehabil.* **74** 347–54

[4] Taub E, Uswatte G and Pidikiti R 1999 Constraint-induced movement therapy: a new family of techniques with broad application to physical rehabilitation—a clinical review *J. Rehabil. Res. Dev.* **36** 237–51

[5] Whiteley J P 2007 Physiology driven adaptivity for the numerical solution of the bidomain equations *Ann. Biomed. Eng.* **35** 1510–20

[6] Chae J, Sheffler L and Knutson J 2008 Neuromuscular electrical stimulation for motor restoration in hemiplegia *Top. Stroke Rehabil.* **15** 412–26

[7] Kimberley T J *et al* 2004 Electrical stimulation driving functional improvements and cortical changes in subjects with stroke *Exp. Brain Res.* **154** 450–60

[8] Hesse S *et al* 2003 Robot-assisted arm trainer for the passive and active practice of bilateral forearm and wrist movements in hemiparetic subjects *Arch. Phys. Med. Rehabil.* **84** 915–20

[9] Casteels C *et al* 2010 *In vivo* type 1 cannabinoid receptor mapping in the 6-hydroxydopamine lesion rat model of Parkinson's disease *Brain Res.* **1316** 153–62

[10] Volpe B T *et al* 1999 Robot training enhanced motor outcome in patients with stroke maintained over 3 years *Neurology* **53** 1874–6

[11] Aasprang A *et al* 2008 Health-related quality of life before and one year after operation for morbid obesity *Tidsskr. Nor. Laegeforen.* **128** 559–62

[12] Caporale N and Dan Y 2008 Spike timing-dependent plasticity: a Hebbian learning rule *Annu. Rev. Neurosci.* **31** 25–46

[13] Cooper S J and Donald O 2005 Hebb's synapse and learning rule: a history and commentary *Neurosci. Biobehav. Rev.* **28** 851–74

[14] Florian R V 2007 Reinforcement learning through modulation of spike-timing-dependent synaptic plasticity *Neural Comput.* **19** 1468–502

[15] Kandel E R 2000 Cellular mechanisms of learning and the biological basis of individuality *Principles of Neural Science* ed E R Kandel, J H Schwartz and T M Jessell (New York: McGraw-Hill) pp 1247–79

[16] van Rossum M C, Bi G Q and Turrigiano G G 2000 Stable Hebbian learning from spike timing-dependent plasticity *J. Neurosci.* **20** 8812–21

[17] Daly J J *et al* 2009 Feasibility of a new application of noninvasive brain computer interface (BCI): a case study of training for recovery of volitional motor control after stroke *J. Neurol. Phys. Ther.* **33** 203–11

[18] Prasad G *et al* 2010 Applying a brain–computer interface to support motor imagery practice in people with stroke for upper limb recovery: a feasibility study *J. Neuroeng. Rehabil.* **7** 60

[19] Broetz D *et al* 2010 Combination of brain–computer interface training and goal-directed physical therapy in chronic stroke: a case report *Neurorehabil. Neural Repair* **24** 674–9

[20] Bai O *et al* 2008 A high performance sensorimotor beta rhythm-based brain–computer interface associated with human natural motor behavior *J. Neural Eng.* **5** 24–35

[21] Medical Research Council of the United Kingdom 1978 Aids to the examination of the peripheral nervous system *Memorandum No 45,* Palo Alto

[22] Gladstone D J, Danells C J and Black S E 2002 The Fugl–Meyer assessment of motor recovery after stroke: a critical review of its measurement properties *Neurorehabil. Neural Repair* **16** 232–40

[23] Oostenveld R and Praamstra P 2001 The five percent electrode system for high-resolution EEG and ERP measurements *Clin. Neurophysiol.* **112** 713–9

[24] Blankertz B *et al* 2007 The non-invasive Berlin brain–computer interface: fast acquisition of effective performance in untrained subjects *Neuroimage* **37** 539–50

[25] Guger C, Ramoser H and Pfurtscheller G 2000 Real-time EEG analysis with subject-specific spatial patterns for a brain–computer interface (BCI) *IEEE Trans. Rehabil. Eng.* **8** 447–56

[26] Chen C F *et al* 2010 Screening of dengue virus in field-caught Aedes aegypti and Aedes albopictus (Diptera: Culicidae) by one-step SYBR green-based reverse transcriptase-polymerase chain reaction assay during 2004–2007 in Southern Taiwan *Vector Borne Zoonotic Dis.* **10** 1017–25

[27] Guyon I *et al* 2002 Gene selection for cancer classification using support vector machines *Mach. Learn.* **46** 389–422

[28] Schroder M *et al* 2005 Robust EEG channel selection across subjects for brain–computer interfaces *EURASIP J. Appl. Signal Process.* **19** 3103–12

[29] Kwok T and Smith K A 2000 Experimental analysis of chaotic neural network models for combinatorial optimization under a unifying framework *Neural Netw.* **13** 731–44

[30] Efron B 1987 Better bootstrap confidence intervals *J. Am. Stat. Assoc.* **82** 171–85

[31] Allison B Z *et al* 2010 Toward a hybrid brain–computer interface based on imagined movement and visual attention *J. Neural Eng.* **7** 26007